atmosphere

MDPI

Article

Modeling the Airborne Transmission of SARS-CoV-2 in Public Transport

Christina Matheis [1,*], Victor Norrefeldt [1], Harald Will [1], Tobias Herrmann [2], Ben Noethlichs [2], Michael Eckhardt [3], André Stiebritz [3], Mattias Jansson [3] and Martin Schön [3]

[1] Department of Energy Efficiency and Indoor Climate, Fraunhofer Institute for Building Physics IBP, Fraunhoferstr. 10, 83626 Valley, Germany; victor.norrefeldt@ibp.fraunhofer.de (V.N.); harald.will@ibp.fraunhofer.de (H.W.)
[2] IFB (Institute for Railway Technology), Carnotstr. 6, 10587 Berlin, Germany; he@bahntechnik.de (T.H.); bn@bahntechnik.de (B.N.)
[3] Alstom, Am Rathenaupark 1, 16761 Hennigsdorf, Germany; michael.eckhardt@alstomgroup.com (M.E.); andre.stiebritz@alstomgroup.com (A.S.); mattias.jansson@alstomgroup.com (M.J.); martin.schoen@alstomgroup.com (M.S.)
* Correspondence: christina.matheis@ibp.fraunhofer.de

Abstract: This study presents the transmission of SARS-CoV-2 in the main types of public transport vehicles and stations to comparatively assess the relative theoretical risk of infection of travelers. The presented approach benchmarks different measures to reduce potential exposure in public transport and compares the relative risk between different means of transport and situations encountered. Hence, a profound base for the selection of measures by operators, travelers and staff is provided. Zonal modeling is used as the simulation method to estimate the exposure to passengers in the immediate vicinity as well as farther away from the infected person. The level of exposure to passengers depends on parameters such as the duration of stay and travel profile, as well as the ventilation situation and the wearing of different types of masks. The effectiveness of technical and behavioral measures to minimize the infection risk is comparatively evaluated. Putting on FFP2 (N95) masks and refraining from loud speech decreases the inhaled viral load by over 99%. The results show that technical measures, such as filtering the recirculated air, primarily benefit passengers who are a few rows away from the infected person by reducing exposure 84–91%, whereas near-field exposure is only reduced by 30–69%. An exception is exposure in streetcars, which in the near-field is 17% higher due to the reduced air volume caused by the filter. Thus, it can be confirmed that the prevailing measures in public transport protect passengers from a high theoretical infection risk. At stations, the high airflows and the large air volume result in very low exposures (negligible compared to the remaining means of transport) provided that distance between travelers is kept. The comparison of typical means of transport indicates that the inhaled quanta dose depends primarily on the duration of stay in the vehicles and only secondarily on the ventilation of the vehicles. Due to the zonal modeling approach, it can also be shown that the position of infected person relative to the other passengers is decisive in assessing the risk of infection.

Keywords: simulation; zonal modeling; SARS-CoV-2; public transport; airborne transmission; risk assessment

Citation: Matheis, C.; Norrefeldt, V.; Will, H.; Herrmann, T.; Noethlichs, B.; Eckhardt, M.; Stiebritz, A.; Jansson, M.; Schön, M. Modeling the Airborne Transmission of SARS-CoV-2 in Public Transport. *Atmosphere* **2022**, *13*, 389. https://doi.org/10.3390/atmos13030389

Academic Editors: Ashok Kumar, Amirul Khan, Alejandro Moreno Rangel and Michał Piasecki

Received: 18 January 2022
Accepted: 23 February 2022
Published: 25 February 2022

1. Introduction

During the spread of SARS-CoV-2, it was found that transmission occurs primarily by virus-bearing particles [1–5]—consider the following three routes of transmission for SARS-CoV-2:

1. Direct transmission by droplets >5 µm containing the virus emitted by an infected person.
2. Transmission by respiratory droplets and aerosols (<5 µm) that contain the virus and can remain suspended in the air for an extended time and travel greater distances.

3. Transmission by direct contact with the virus through contact with an infected person or through direct contact with contaminated surfaces.

The difference between droplets and aerosols is the particle size or physical properties. While larger particles (>5 µm) sink to the ground more quickly, the smaller aerosols can remain in the air for a longer time and thus disperse in enclosed spaces. For example, a 5 µm aerosol takes 33 min to sink to ground from 1.5 m in resting air. Whether and how long droplets and aerosols remain suspended in the air depends on various factors such as temperature and humidity [2,6].

In the context of the SARS-CoV-2 pandemic, ways to minimize the risk of infection are constantly being sought. A minimum distance of 1.5 m from another person is recommended to minimize the likelihood of coming into contact with virus-containing droplets from a person infected with SARS-CoV-2 [7]. Partly because these distances cannot be maintained during rush hour, many people have health concerns about using public transportation. Despite implemented hygiene concepts, this has led to a significant decline in passenger numbers. Statistical data in the number of sold tickets in Germany reveal a decrease of 40–70% of passengers after the outbreak of SARS-CoV-2 in 2020 [8]. To counteract this effect, the effectiveness of current protective measures, as already elaborated in [9], is to be examined by means of simulations.

In [10], it is also shown that there is a great demand for research in the transport sector worldwide to counteract this effect. This includes some publications on infections with SARS-CoV-2 in public transport in USA, China, Japan and UK [10]. For example, in a Chinese study, a variety of protection measures in public transportation are developed, ranging from institutional requirements to personal protection and knowledge promotion [11]. However, the effect can only be confirmed in general terms. The authors of [12] conduct a systematic literature review on transmission in trains and buses and conclude that an empirical definition of the risk of infection is lacking observational data. Therefore, a model-based estimation of the risk based on the interior air, the travel duration and the passenger density is considered a beneficial approach. In [13], elaborate CFD flow simulations are performed in a car to determine infection risk. It is found that zero-dimensional approaches have limited applicability for an adequate assessment of risk in confined spaces, and that multidimensional approaches are necessary to represent complex fluid dynamics. The detailed consideration, however, does not allow the results to be transferred to other means of transport [13]. An approach to risk assessment in transportation based on simple geometry and the assumption of an ideally mixed space is shown in [14]. Nevertheless, these methods do not allow for a detailed comparison of all occupied areas in public transport taking into account airflows. In an experimental study on a train, [15] concludes that the carriage is not well mixed over its length but rather along its height and width. Hence, the location of a possibly infectious passenger is crucial for the infection risk, and a purely well-mixed assumption is not valid. Similar to these findings, virus exposure is considered locally resolved. The calculated exposures provide the basis for assessing the risk of airborne transmission of SARS-CoV-2 in public transportation and for evaluation of measures and recommendations. Here, the focus lies in understanding the dispersion of SARS-CoV-2 in indoor air and quantifying it assuming a SARS-CoV-2 infected passenger is on a train, bus or in a train station. Scenarios are simulated with adherence to the behavioral recommendations, such as wearing masks, avoiding speech and maintaining distances. The influence of ventilation in respect to fresh air rates and filtration efficiencies will also be investigated. With regard to a return to normality, scenarios without these measures are also considered.

A represented selection of the most important vehicle types of German public transport is being taken into account: long-distance trains and long-distance buses, regional trains, suburban trains, city trains and subway trains, streetcars and city buses. Furthermore, stations and stops are modeled both above and below ground. For model validation, CO_2 measurements were used as field measurements in public transport, from which fresh air volumes can be back-calculated and verified against manufacturer data. In a previously

performed literature study, typical vehicle categories, information on possibilities and limitations of the system technology, information on aerosol dispersion, data on passenger numbers before and after start of the pandemic and documented transmissions of SARS-CoV-2 in public transport were determined and used for the simulations [16]. Through this approach, the gap can be closed between cited measurements or simulations for specific coaches and ventilation situations and the broad overview of meta-studies.

2. Materials and Methods

The applied modeling methodology is based on a zonal model, which is used to describe the indoor airflow [17]. In the model, a passenger infected with SARS-CoV-2 is inserted as a source. Starting from this, the dispersion behavior in different trains, buses and station types is determined. The main features of the modeling approach are presented below.

2.1. Zonal Model

The "Indoor Environment Simulation Suite" is a toolbox of different sub-models for the rapid simulation of indoor climate. The core of this toolbox is the "Velocity Propagating Zonal Model" (VEPZO) [17], which in many cases is a superior alternative to complex computational fluid dynamics (CFD) simulations. A trade-off between computational effort and level of detail of the result is chosen. It uses similar mathematical theories but divides the space into only 100 to 1000 volume zones [17]. Especially for considerations such as temperature and concentration fields in the interior, zonal modeling can achieve informative value similar to the detailed CFD simulations, but at lower computational cost. Therefore, the zonal modeling approach can be used for parametric studies. The model has been developed in the multi-physics modeling language Modelica [18], and the commercial software Dymola is used for solving of the model equations.

The VEPZO volume model implements the conservation of scalar quantities, such as mass, heat and tracer gas and particle/aerosol concentrations. Neighboring zones are connected by flow models in which the amount of exchanged air is calculated. By arranging the volume and flow models in three dimensions, space is represented zonally (Figure 1) to predict temperature, mass and airflow distribution.

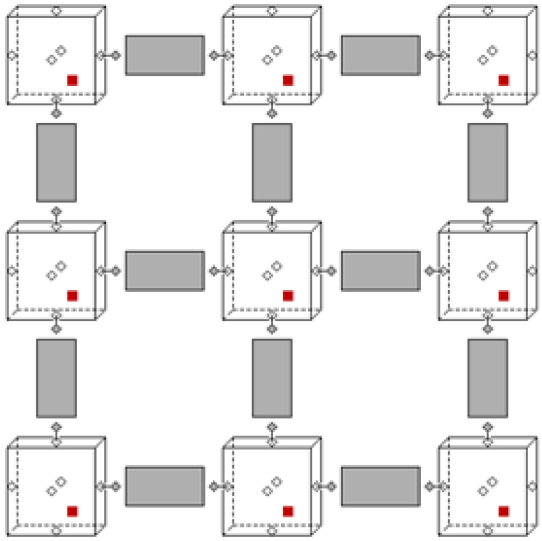

Figure 1. Schematic 2D representation of a zonal model: subdivision of the space into zones (cubes) connected by flow models (grey).

A detailed description of the zonal approach comprising the flow and volume models can be found in [17]. In the volume model, the equations for conservation of mass, heat and tracer gases are set up. For mass conservation, the air volumes flowing across the six zonal

boundaries (right, left, front, back, down and up) are added. In a steady state, the sum of all inflowing and outflowing air quantities is zero. For heat conservation, the internal loads and the enthalpies flowing across the zone boundaries are summarized in Equation (1) [17]. This results in the transient profile of the enthalpy. The temperature can be determined via the equations of the state of the air:

$$V_i \cdot \rho_i \cdot \dot{h}_i = \sum_{j=1}^{6} \dot{m}_j \cdot h_{i/j} + \sum \dot{Q}_{Source} \quad (1)$$

where V_i, ρ_i, $\dot{h}_i$ is volume, density and enthalpy change of zone i; $\dot{m}_j$ is mass flow from the adjacent zone (positive: inflowing, negative: outflowing); $h_{i/j}$ is enthalpy of zone i or j, depending on flow direction; $\dot{Q}_{Source}$ is heat flow from sources, e.g., heat emission from persons, convective exchange with enclosing surfaces, etc.

The conservation equations for tracer gases, particles and aerosols in the air are implemented analogously to enthalpy conservation. Since emitted human viral particles have been shown to be capable of remaining airborne for extended periods [19], deposition was not considered in the simulation. This approach is considered conservative. In common zonal models, the airflow between two zones is calculated using the Bernoulli equation. In the VEPZO model, however, the acceleration of the flow in the flow paths is calculated in order to avoid the numerically unstable square root function of velocity vs. pressure difference. To model the losses of the flow, a viscous term is introduced. The flow model takes into account the air fluxes between the neighboring zones and calculates the mass flow to be exchanged via the pressure, momentum, height difference and the viscous loss term. The effective viscosity is a calibration parameter of the model, and it has been concluded that 0.001 provides good results [17]. To calculate the flow velocity, Equation (2) sums up the forces acting on the flow path and determines the resulting acceleration of the flow. The equation underlying the flow path is shown for the x-coordinate but is correspondingly valid for the other Cartesian coordinates:

$$\dot{u} = -\frac{\Delta p_{i,j} + \Delta\left(u^2\right)_{i,j} + g \cdot \Delta z_{i,j}}{\Delta x} + \frac{\mu}{\rho} \cdot \left(\frac{\Delta \frac{\partial u}{\partial y}}{\Delta y} + \frac{\Delta \frac{\partial u}{\partial z}}{\Delta z} \right) \quad (2)$$

where $\dot{u}$ is acceleration of air in the x-direction (in the steady state 0); $\Delta p_{i,j}$, $\Delta\left(u^2\right)_{i,j}$ and $\Delta z_{i,j}$ are pressure difference, difference of velocity squares and height difference, respectively, between zones i and j; g is 9.81 m/s^2; ρ is density of flowing air; μ is calibration parameter for effective viscosity (0.001).

2.2. Model Development and Evaluation

The Thermal Model Generation Tool is a self-developed tool used for model generation [20]. Starting from a geometry file of the simulated interior, the zoning in x-, y- and z-directions is defined, and the location of flow sources and sinks as well as heat loads are determined. The tool then automatically generates the Modelica source code of the zonal model. After defining the source intensities and the thermal resistances of enclosures, the exported model is ready for simulation. The described workflow is shown in Figure 2.

The airborne exposure to potentially infectious material inside vehicles and at stations was evaluated in particular. To represent the airborne SARS-CoV-2 spread, the so-called quanta notion was used. This is a description of the amount of virus emitted by a person infected with SARS-CoV-2 and is based on [21,22]. By definition, a vulnerable person has a 63% risk of getting infected after inhaling the dose of one quanta. This definition was set out for the initial SARS-CoV-2 virus, to the best of our knowledge, how mutations change this rate is not defined. The advantage of this approach is that, regardless the dominant mutation of SARS-CoV-2 or any other airborne infectious disease, the general conclusions on protective means and their efficiency remain valid. Therefore, the theoretical

risk assessment in this study is based on the inhaled quanta-dose. The calculated quanta concentration is exported as a result for each individual zone and presented as a numerical value. In addition, the concentration predicted in simulation is deposited as a color gradient, as shown in Figure 3, from green (from 0 mili-quanta/m^3) to yellow (at 20 mili-quanta/m^3) to red (from 50 quanta/m^3).

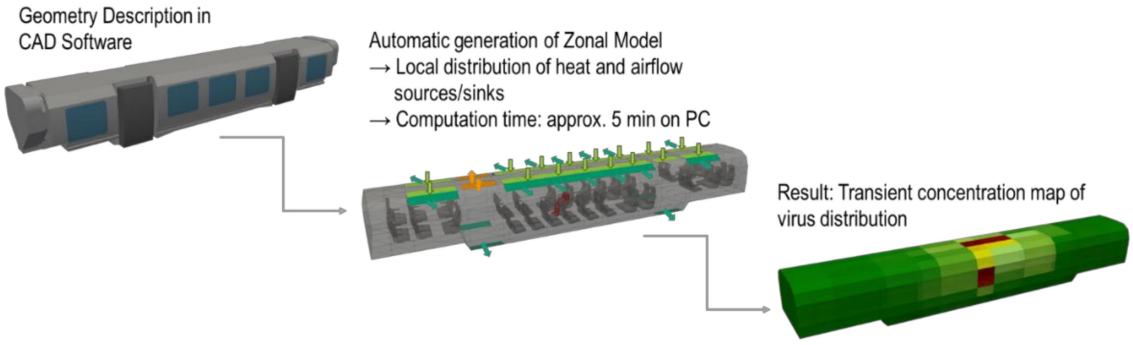

Figure 2. Indoor Environment Simulation Suite (IESS) workflow.

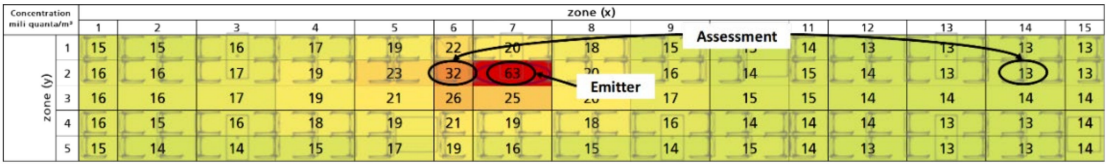

zone (y) \ zone (x)	1	2	3	4	5	6	7	8	9	11	12	13	14	15
1	15	15	16	17	19	22	20	18	15	14	13	13	13	13
2	16	16	17	19	23	32	63	20	16	14	15	14	13	13	13
3	16	16	17	19	21	26	25	20	17	15	15	14	14	14	14
4	16	15	16	18	19	21	19	18	16	14	14	14	13	13	14
5	15	14	14	15	17	19	16	15	14	15	14	13	13	13	14

Figure 3. Example of evaluation/representation of the simulation: shown is the concentration in mili-quanta/m^3 in a section through the compartment at breathing height.

The inhaled dose at selected locations is determined by integrating the concentration over the residence time, weighted by the respiratory volume and the protective effect of masks, as shown in Equation (3). The neighboring zone of the emitter with the highest concentration (max. dose) and a zone far away from the emitter (min. dose) are evaluated in each case. As a measure for the dose, the mili-quanta is used, where 1000 mili-quanta correspond to one quanta.

$$Dose = \dot{V}_{Breathing} \cdot f_{Mask} \cdot \int_{t_{start}}^{t_{end}} c_i(t)dt \quad (3)$$

where $\dot{V}_{Breathing}$ is breathing volume, here 540 L/h (light, sedentary work, [23]); f_{Mask} is self-protection effect depending on mask type (Section 2.3 Boundary Conditions); $c_i(t)$ is time-resolved course of concentration in the evaluated zone i; t_{start} and t_{end} are start and end of exposure, respectively.

2.3. Boundary Conditions

2.3.1. Viral Load

In the following, a theoretical risk of infection is assumed for everyone present in the vehicles without knowledge of personal risk factors. To assess whether an infectious human should be modeled by aerosol, particle or quanta emission rates, a comparison in Figure 4 was performed [16].

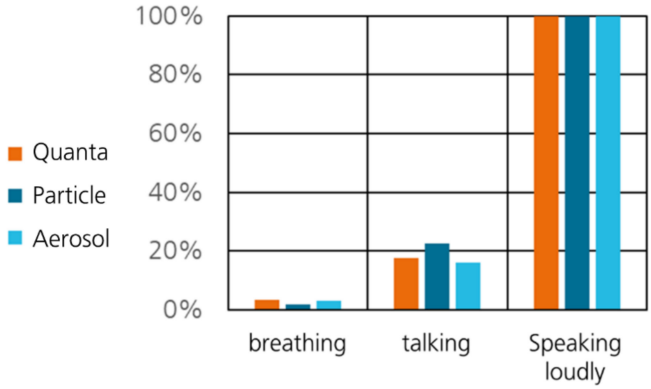

Figure 4. Relative comparison of approaches to describe the emitter as a quanta, particulate or aerosol source.

Speaking loudly corresponds to 100%. Depending on the observation, breathing equals 2–4% of the emissivity of speaking loudly and talking equivalent to 16–23%. Thus, an approximately constant gradation between activity levels is expected independent of the selected source term. The relative proportions between breathing, talking and speaking loudly are quite close (Table 1). That is, regardless of how the source is modeled, the relative outcome between the different activity levels remains similar.

Table 1. Comparison of the source description of the emitter.

	Quanta		**Particle**		**Aerosol**	
Literature	[24]	[21,22]	[25]	[26]	[23]	[27]
Breathing	2.3 quanta/h	Double logarithmic plots and information on percentiles	0.1 particle/s	Normal: 14–71 particle/L	0.0018 mL/m^3	Online calculator, based on [23], use of a stochastic approach for risk assessment.
Talking	11.4 quanta/h		1.2 particle/s		0.0096 mL/m^3	
Speaking Loudly	65.1 quanta/h		5.3 particle/s Max.: 17 particle/s		0.06 mL/m^3	
Super Emitter	factor 10^2		660–3230 p/L (factor 10^2)	660–3230 p/L (factor 10^2)	no	
Assessment	Introduced specifically for SARS-CoV-2 Allows super emitter assessment Theoretical risk assessment		Reference literature is not SARS-CoV-2 specific. Divergent data on super emitters.		No information on super emitters. Theoretical risk assessment derived, specifically introduced for SARS-CoV-2.	

The quanta doses recorded in different scenarios are compared with the assumption that a higher dose intake always leads to a higher risk. The emission strength is given in quanta/h for different activity levels. An Excel calculation tool [24] fixed the following listed mean emission rates:

1. Breathing: 2.3 quanta/h
2. Talking: 11.4 quanta/h
3. Speaking loudly: 65.1 quanta/h

These values are implemented as a unidirectional source in the model.

2.3.2. CO_2 Emission

For model validation against in situ measurements, it was necessary to use an airborne tracer that is commonly found in transport vehicles. CO_2 is a reliable tracer gas emitted by passengers and thus allows, together with the passenger count, an estimation of the fresh airflow rate supplied to the cabin. To measure the CO_2 concentration in transport means, a Rotronic CP11, 0–5000 ppm with accuracy of ±30 ppm/±5% was used. Passengers were accurately counted where feasible (especially in long-haul transport) or estimated (e.g., quarter filled, half full, especially in local transport). For model validation an emission rate of 18 L/h is assumed per passenger [28].

2.3.3. Masks

Wearing masks is considered an effective measure to reduce the spread of SARS-CoV-2. A recent review [29] also recommended the wearing of masks in public places. Therefore, the following three mask types were included in simulations:

1. without mask
2. mouth-nose protection (MNP) and homemade masks
3. FFP2-mask

In each case, the simulation of mask types includes the protective effect during exhalation (i.e., a percentage reduction in the source term) and the protective effect during inhalation (i.e., a reduction in the absorbed dose). Average values for the mask types are considered in the simulations as given in Table 2, however, a higher protective effect [24,30] can be achieved with correct handling. To compare the three different mask types, it is assumed that everyone in the vehicle or on the station wears the same mask type.

Table 2. Reduction effect through masks [31].

Mask Type	Reduction Exhalation	Reduction Inhalation
without	0%	0%
(MNP) or homemade mask	50%	30%
FFP2 (N95) mask	90%	90%

2.3.4. Ventilation

Depending on the operational condition, different modes of ventilation are implemented in the models. Generally, the supply air in public transport is a mixture of fresh air, which is free of SARS-CoV-2 pathogens, and recirculated air, with the viral load of the return air of the vehicle. Typical filters used today on trains are not of sufficient quality for viral particles. In the case studies, hypothetical filter implementations were considered, taking into account that changing the filter to HEPA in an existing system will lead to reduced flow. In the model, the filter is described as a sink with a certain efficiency, i.e., the viral load downstream is reduced by a factor from the upstream load. The magnitude of flow reduction and realistically achievable filter efficiencies was provided by experts within the research group. Any filtering and purification devices reduce the pathogen concentration in the recirculated air by a certain percentage. For example, if a filtering effect of 80% is assumed, the recirculated air in the model will have a residual pathogen concentration of 20% compared to the exhausted air.

In addition, the air exchange through the open doors is implemented in the model. The main driver for this is the temperature difference between the interior and the outside air. When the door is opened, this causes cool air to enter the cabin through the lower area of the door, while warmer air leaves the cabin through the upper area. The formulas for temperature-driven air exchange at a rectangular opening are derived from [32].

$$\dot{V}_{door} = \frac{1}{3} \cdot C_D \cdot B \cdot \sqrt{\frac{\Delta T \cdot g \cdot H^3}{T_m}} \tag{4}$$

where $\dot{V}_{door}$ is volume flow through the open door; B is width; H is height; ΔT is temperature difference; T_m is mean temperature; g = 9.81 m/s^2; C_D = pressure loss coefficient.

C_D is the pressure loss coefficient and ultimately describes the flow resistance of the door opening. As a typical, conservative assumption, the value of C_D is considered as 0.4. The indoor temperature of 23 °C, the outdoor temperature of 16.6 °C for the summer and 9.1 °C for winter (Germany-wide average) is assumed [33]. The outdoor temperature in the subway tunnel was estimated to be 15 °C based on measurement (27 January 2021, Munich, Sendlinger Tor subway station). The airflow calculated by Equation (4) during the door opening times serves as input for a ventilation source in the model.

Openable windows were not modeled. Since the infection situation is most critical in winter, windows are usually closed at this time of year for comfort and energy efficiency reasons. If a window is opened in practice, additional air exchange takes place, which results in a lower risk of infection. The simulations thus correspond to a worst-case scenario. In addition, their shape varies greatly, and the actual opening is difficult to model in practice.

2.3.5. Partition Walls

Partition walls as flow obstacles are implemented in the model by reducing the cross-section area of the geometrically closest flow path. In the case of an airtight partition, the corresponding flow path and thus the air exchange between the affected, neighboring zones are removed from the model. Thus, seat surfaces and backrests that affect the airflow are considered in the model.

2.3.6. Occupancy Density

The occupancy density is used as a parameter for heat release in the interior. For air conditioning and ventilation systems operated in fixed-volume flow mode, the occupancy density does not influence the supply airflowrate. In demand-controlled systems (e.g., the high-speed train ICE), the fresh air volume adjusts to the occupancy. For the passenger density at the stations, it is assumed that there is a train on each side of the platform. The number of people is therefore made up of the passengers who get on or off both trains at the same time. A typical capacity utilization of the trains in pandemic periods was applied [16]. Simulations focus on the airborne spread of infectious matter, hence it is intrinsically assumed that the distance between passengers is large enough to inhibit direct particle transmission.

2.4. Determination of Train, Bus and Station Types

In order to make a representative selection of train types, a survey was carried out on the number and characteristics of the train stock in Germany [16]. Furthermore, the selection was based on the availability of operational data and the possibility to conduct validation measurements on the modeled vehicles. Table 3 shows the selected types and the criteria by which these types where chosen. In cases where no detailed data on ventilation were available, data from these measurements were used and determined using CO_2 balancing equations.

Table 3. Representative trains, buses and stations based on research and statistical analysis.

Means of Transport	Type	Selection Criterion	Literature
Long-Distance Train	ICE high-capacity train	Most common type	[34–36]
Regional Train/Local Traffic	multiple-unit train TALENT 2/3 (Bombardier Transportation)	Very common type, Detailed data basis	[34–36]
Subway/Light Rail Vehicles	Munich subway (A series) Munich subway (C series)	Most common length (15 to 30 m) Future increase in frequency expected	[37]
Tram/Streetcar	Flexity Berlin (Bombardier Transportation)	Most common length (30 m)	[37–40]
Suburban Train	TALENT 2 (Bombardier Transportation)	Typical vehicle dimensions, Detailed data basis	-
City Bus	12 m Bus	Most common type, Length	[40]
Long-Distance Bus	FDH2 bus	Possibility of in situ measurements	[41]
Station	Subway platform in low position with central platform, station concourse of terminus station (half-open)	Most common platform type for subway, limiting case (underground)	

If similar ventilation systems are installed for the train types not considered here, the simulated results can also be transferred to these. For this purpose, the fresh and recirculated air volumes, the form of air injection and the driving cycle must be compared with the input data used here.

As an estimate of whether the distance of 1.5 m can be maintained to exclude transmission by large particles, the maximum occupancy density possible for this purpose is determined. A circle of 1.5 m diameter requires an area of 1.76 m^2. It corresponds to a maximum occupancy density of 0.56 passengers/m^2, neglecting areas that cannot be used by passengers. The number of passengers for the considered means of transport in the pre-pandemic phase was ascertained from German operator data [42–48] and statistical information [8]. The reduction of travelers during the pandemic was determined from [16]. In general, it can be assumed that the minimum distance of 1.5 m can only be maintained in selected cases, such as in low-occupancy vehicles at night or on secondary routes. For this reason, it is deemed necessary to wear a medical mask or mouth-nose protection (MNP). Both terms are used synonymously in the following. Additionally, simulation cases with stronger-filtering FFP2 masks were included to take into account that some regions impose this type of mask.

3. Simulation

In the simulation, it is assumed that an infected person is present in the transport vehicle or on the platform. Based on this, the exposure in the near field and in the wider environment of the emitter is calculated. The virus is assumed to be airborne. Pathogen transmission through surfaces (smear infection) is not modeled because findings consistently show only low levels of viral load on surfaces [16].

The simulation study included eight different means of public transport and two types of train stations, with the typical travel time determined for the respective means of transport. The typical maximum time spent on the platform (8 to 35 min) was taken from [49]. The models and corresponding input data were validated with existing manufacturer data or by CO_2 measurements. In each case, the evaluation is performed concerning the activity (breathing, talking and loud speaking) of the SARS-CoV-2 infected passenger and by mask type (without mask, MNP and FFP2). Then the influence of air filtration and the amount of fresh air is considered. In addition, the heating and cooling scenarios in the respective means of transport are examined to observe a possible influence on the airflow pattern. The effect on exposure of introducing compartments in comparison to the saloon coach was also investigated.

3.1. Input Data

For zonal modeling, the geometry of the selected means of transport are divided into small zones. Depending on the geometry and interior design, 8–17 zones in the x-direction (longitudinal) and 4–5 zones in the y-direction were created. The height is divided into five zones in each case (cf. Figure 5). In comparison, the zones in the models of stations are significantly larger to represent areas shown in Figure 6. The zones surrounding the emitter are 5 m long in their largest extension.

In heating mode, the air is supplied mainly through the floor area and is extracted through the ceiling. In cooling mode, air is supplied from the ceiling (cf. Figure 5). This results in different flow characteristics in the coaches. Depending on the train type, recirculation air is aspired in a dedicated outlet or from the exhaust air ducting. According to the operators, no distinction is made between heating and cooling cases in buses and tramways.

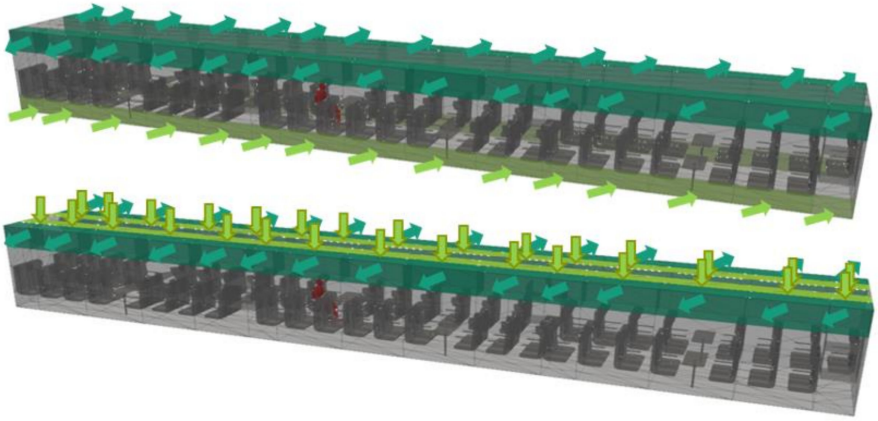

Figure 5. Zonal model of the ICE 4 with sources and sinks for heating (**top**) and cooling (**bottom**) mode: light green arrows, supply air; dark green arrows, exhaust air; red-marked person, emitter.

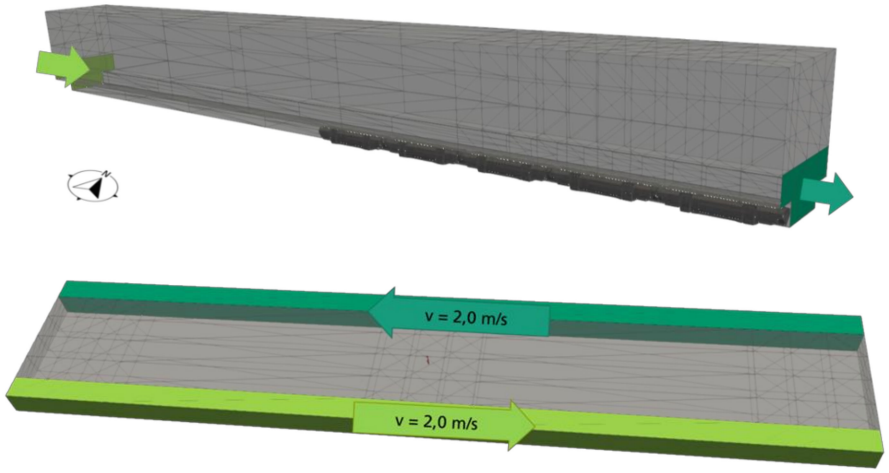

Figure 6. Simulation models of the train hall section (**top**) and an underground station using the example of Munich Central Station and the Odeonsplatz (U3/U6 subway station) in Munich (**bottom**).

For the train station hall, two cases were considered as flow boundary conditions. One case is characterized by the mean wind speed from the direction NW to SW at 3.3 m/s according to reference weather data in Munich [33]; the other case is purely thermally driven, with an assumed temperature difference of 1 K. This is an assumption. However, it is expected that waste heat from trains, lighting and passengers, as well as solar heat input may well lead to an increase in temperature in the building. The formula according to [32] was again used to determine the resulting airflowrate. For the evaluation of a subway station, a mean flow velocity through the two tunnel tubes of 2 m/s was assumed as a boundary condition. This value is the time average of any flows created by the stack effect and the piston ventilation effect that incoming trains have (Z. Kebdani, personal communication, 5 February 2021) [50].

To consider the effects of door opening in the simulations, travel profiles for the various means of transport were derived (Table 4):

Table 4. Typical travel profiles and durations of stay in the different means of transport and stations.

Means of Transport	Stop Time	Travel Time between Stations	Total Travel Duration	Literature
Long-Distance Train	negligible	2.5 h	2.5 h	Measurement period during validation
Regional Train/Local Traffic	52 s (1 door)	295 s	98 min	Research on travel and stop times
Subway/Light Rail Vehicles	25 s (3 doors)	72 s	29.5 min	Research on travel and stop times [48,51]
Tram/Streetcar	17 s (2 doors)	65 s	25 min	Research on travel and stop times
Suburban Train	36 s (2 doors)	127 s	77 min	Research on travel and stop times
City Bus	12 s (2 doors)	70 s	21.5 min	Research on travel and stop times
Long-Distance Bus	negligible	2.5 h	2.5 h	Comparability with long-distance train
Stations	-	-	12–35 min (depending on reason for travel and time of day)	[49]

3.2. Validation

The models were validated using measured CO_2 concentrations from field measurements. For example, measurement was carried out on the Munich–Erfurt route in an ICE 4 to validate the long-distance train (Figure 7). Shortly before Erfurt, the trains pass through a tunnel, where the fresh air supply is interrupted to avoid the pressure surge in the cabin. Figure 7 shows the measured (black, dashed) and simulated (black, solid) CO_2 concentration. Overall, there is good agreement between simulation and measurement, with a maximum deviation of about 150 ppm at time 60 min. Later, it was found that there is also a tunnel at that time, shortly before Nuremberg, which could lead to the measured CO_2 peak.

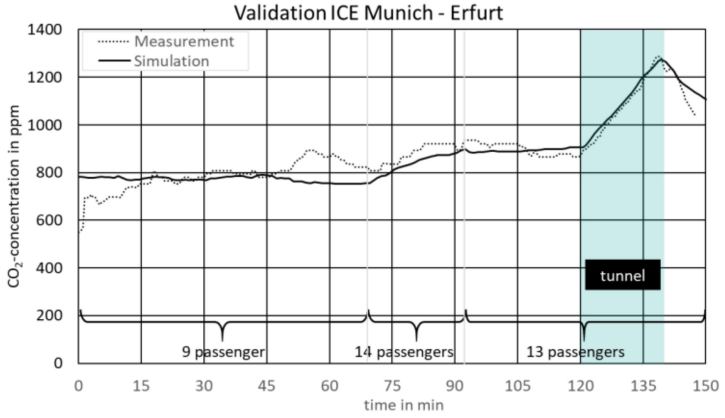

Figure 7. Comparison of measured and simulated CO_2 concentration on Munich–Erfurt route in an ICE 4.

The validation of the remaining models was performed similarly to the long-distance train. The occupancy in the means of transport during the measurements was estimated based on recordings of the measurement team. The actual amount of fresh air was determined based on CO_2 measurements and occupancy. The validation of the zonal model of the regional train and the suburban railroad was carried out based on extensive flow simulations by the manufacturer, Bombardier Transportation. It could be shown in all models that the zonal simulation approach used here is suitable to represent the temperature distribution and thus the indoor climate in the train. For the validation of the above-ground

station, CO_2 concentration was measured at the Munich Central Station. However, the measured values were so close to the outside air that a meaningful validation is impossible.

3.3. Main Results of Flow Simulations

The activity levels of breathing, speaking and speaking loudly, without a mask or with a MNP or FFP2 mask were considered. A concentration profile was created for each simulation. Figure 8 shows an example of the concentration distribution in the horizontal section at head height (approx. 1.1 m) of an ICE large-capacity coach for the case of a speaking infected passenger in the case of HVAC heating at 50% occupancy. It is clear that around the emitter (zone marked with a red oval), there is a higher concentration of up to 32 mili-quanta/m^3, while farther away in the wagon it is 13 to 19 mili-quanta/m^3. The reason for the presence of some infectious material in the distant field is the shape of recirculated air because of the ventilation in the coach.

Concentration in mili-quanta/m³	zone (x)														
	1	2	3	4	5	6	7	8	9	10	11	12	13	14	15
zone (y) 1	15	15	16	17	19	22	20	18	15	13	14	13	13	13	13
2	16	16	17	19	23	32	63	20	16	14	15	14	13	13	13
3	16	16	17	19	21	26	25	20	17	15	15	14	14	14	14
4	16	15	16	18	19	21	19	18	16	14	14	14	13	13	14
5	15	14	14	15	17	19	16	15	14	15	14	13	13	13	14

Figure 8. Example of concentration distribution in mili-quanta per m^3 for the case "HVAC heating, 50% occupancy, talking, without mask" in ICE.

Integrating the concentration from Equation (3) throughout the trip yields the determined inhaled dose. For each simulated case, the minimum dose farther away and the maximum dose at the seats adjacent to the infected passenger are evaluated.

Figure 9 represents the results of minimum and maximum inhaling of infectious material in different speaking and mask wearing scenarios after 2.5 h in an ICE. Without wearing masks, the maximum doses are columns 1, 2 and 3 for breathing, speaking and loud speaking, respectively. The worst-case scenario of loud speaking is considered for MNP and FFP2 masks, where the maximum doses are columns 4 and 5, respectively. For the FFP2 mask, the massive reduction in values is due to pathogen filtering during both exhalation and inhalation. These ratios are valid for all types of transport means and stations.

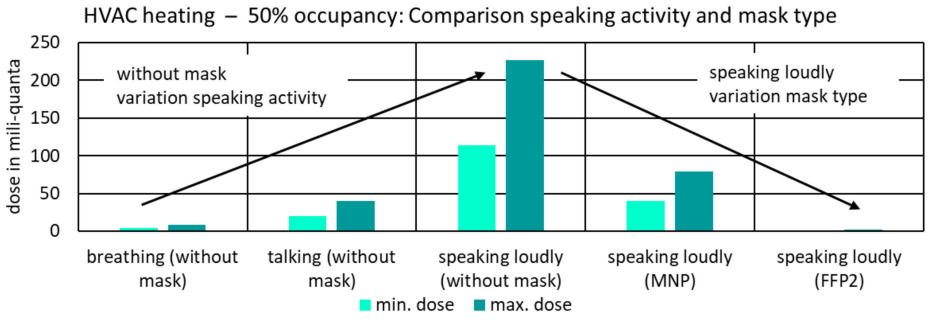

Figure 9. Comparison of inhaled dose in mili-quanta after 2.5 h in ICE with an infected person during different activities (breathing, talking or speaking loudly) of the emitter and with different mask types (none, MNP or FFP2): min. dose, minimum dose absorbed farther away from the emitter; max. dose, maximum exposure that is absorbed close to the emitter.

A comparison of the different ventilation scenarios shows in all means of transport that a similar maximum dose is reached in the vicinity of the emitter with the same supply air quantities. Farther away from the infected person, however, the minimum dose increases as the proportion of outdoor air decreases. The Figure 10 shows the inhaled doses at different

ventilation rates as an example case for the ICE. Here, for example, a demand-driven reduction in the fresh air rate from 1500 m^3/h to 500 m^3/h due to lower occupancy results in a 3.4-fold increase in exposure farther away. In contrast, ventilation with pure, fresh air leads to a 90% reduction in exposure farther away from the emitter.

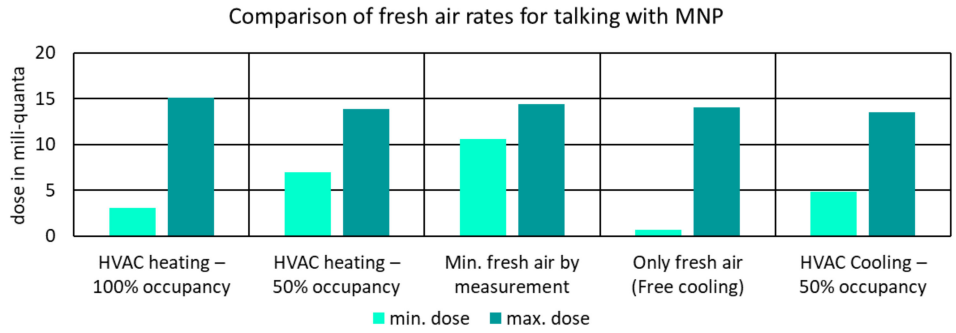

Figure 10. Influence of fresh air and recirculated airflowrate on the amount of exposure for the ICE: min. dose, minimum dose absorbed farther away from the emitter; max. dose, maximum exposure that is absorbed close to the emitter.

For the consideration of recirculating filtered air, a filter effectiveness of 80% towards SARS-CoV-2 was assumed in accordance with the current state of technology. As a result of the increased pressure drop across the filter, there is an assumed reduction in air volumes of 10%. Figure 11 shows the reduction of the exposure due to filtration.

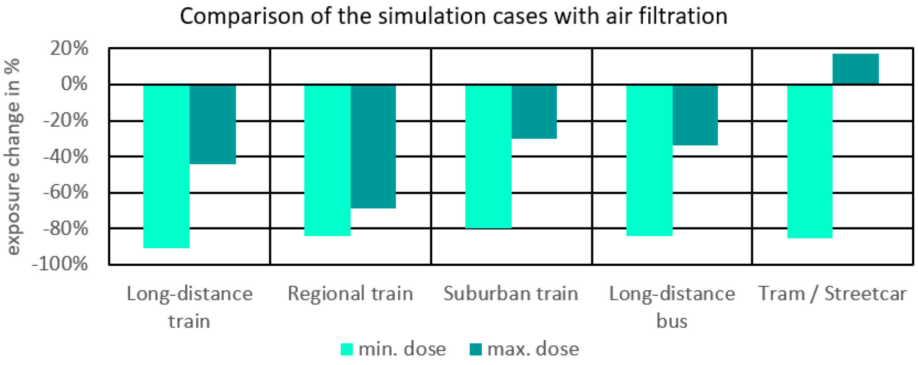

Figure 11. Influence of filtering on the amount of exposure: min. dose, minimum dose absorbed farther away from the emitter; max. dose, maximum exposure that is absorbed close to the emitter.

In the areas farther away from the infected person, the reduction of the inhaled quanta amount is between 80% and 90% in all cases. In the close-up area, the supply of fresh air has a significant influence on the quanta concentration in the air. The better the area is ventilated, the more the emissions can be diluted and the concentration decreases. In the case of streetcar ventilation, at 34%, the proportion of recirculated air is the lowest in comparison with the other vehicles. Here, the main effect is the lower amount of supply air in case of filtering in the close range of the infected person. The emissions are less diluted, resulting in an increase of the quanta dose in the vicinity.

Table 5 presents the inhaled dose for breathing activity of the emitter in the different means of transport. When speaking loudly, the values from Table 6 are obtained. For the comparison of the individual means of transport, the worst-case heating scenario with minimum fresh air supply was selected. In the case of the train station hall, the unfavorable case of thermal-buoyancy-driven flow by a 1 K temperature difference is chosen for comparison.

Table 5. Absorbed dose in mili-quanta when breathing at close proximity (max. dose) or farther away from the emitter (min. dose) for the assumed durations of stay.

	Without Mask		**With MNP**		**With FFP2-Mask**	
	Min. Dose	**Max. Dose**	**Min. Dose**	**Max. Dose**	**Min. Dose**	**Max. Dose**
Long-Distance Train (2.5 h)	6.09	8.33	2.13	2.96	0.06	0.08
Regional Train/Local Traffic (98 min)	0.97	3.01	0.34	1.05	0.01	0.03
Old/New Subways (29.5 min)	0.07/0.03	1.52/1.52	0.02/0.01	0.53/0.53	0.00/0.00	0.02/0.02
Tram/Streetcar (25 min)	0.16	0.87	0.05	0.30	0.00	0.01
Suburban Train (77 min)	0.30	0.96	0.10	0.33	0.00	0.01
City Bus (21.5 min)	0.41	3.16	0.14	1.10	0.00	0.03
Long-Distance Bus (2.5 h)	3.91	6.24	1.37	2.18	0.04	0.06
Train Station Hall (35 min)	0.00	0.09	0.00	0.03	0.00	0.00
Underground Station (8 min)	0.00	0.04	0.00	0.01	0.00	0.00

Table 6. Absorbed dose in mili-quanta when speaking loudly at close proximity (max. dose) or farther away from the emitter (min. dose) for the assumed durations of stay.

	Without Mask		**With MNP**		**With FFP2-Mask**	
	Min. Dose	**Max. Dose**	**Min. Dose**	**Max. Dose**	**Min. Dose**	**Max. Dose**
Long-Distance Train (2.5 h)	172.47	235.86	60.37	82.55	1.72	2.36
Regional Train/Local Traffic (98 min)	27.49	85.15	9.62	29.80	0.27	0.85
Old/New Subways (29.5 min)	2.01/0.74	43.12/42.95	0.70/0.26	15.09/15.03	0.02/0.01	0.43/0.43
Tram/Streetcar (25 min)	4.41	24.59	1.54	8.61	0.04	0.25
Suburban Train (77 min)	8.45	27.09	2.96	2.48	0.08	0.27
City Bus (21.5 min)	11.62	89.34	4.07	31.27	0.12	0.89
Long-Distance Bus (2.5 h)	110.60	176.64	38.71	61.82	1.11	1.77
Train Station Hall (35 min)	0.05	2.45	0.02	0.86	0.00	0.02
Underground Station (8 min)	0.01	1.10	0.00	0.38	0.00	0.01

3.4. Further Simulations

For a fully occupied long-distance train, the presence of an infected person in a compartment is investigated. For this purpose, walls were introduced in the model around

the emitter's seating group. Due to pressure equalization, overflow is possible through joints or gaps, for example, through doors. It is assumed that a fraction of exhaust air from the compartment is supplied to the rest of the coach by the central air recirculation system. Figure 12 shows the concentration distribution when the emitter speaks loudly without a mask in a compartment. Compared with the large-capacity coach, the concentration peak is confined to the compartment. In the area outside the compartment, the recirculating air is the cause of dispersion, and a result similar to the large-capacity coach is obtained. Figure 13 compares the inhaled dose. Other passengers in the compartment are exposed to a dose almost two times higher than in the large-capacity coach. On the other hand, numerically, fewer persons are affected. The optimum protection for persons outside the compartment would theoretically be achieved by a decentralized air recirculation system, but this would mean that each compartment would need its own ventilation system.

Concentration in mili-quanta/m³		zone (x)														
		1	2	3	4	5	6	7	8	9	10	11	12	13	14	15
zone (y)	1	25	25	26	28	29	37	176	30	27	25	24	24	23	23	24
	2	26	26	27	30	29	41	446	34	29	27	25	25	24	24	24
	3	26	27	28	30	32	37	41			27	26	25	24	24	24
	4	26	26	27	29	31	33	31	33	29	26	25	25	24	24	24
	5	25	24	25	26	27	31	32	29	26	26	26	24	23	23	24

compartment

Figure 12. Concentration distribution in mili-quanta/m^3 for the case "Speaking loudly, without mask" in the ICE with compartment formation around the emitter.

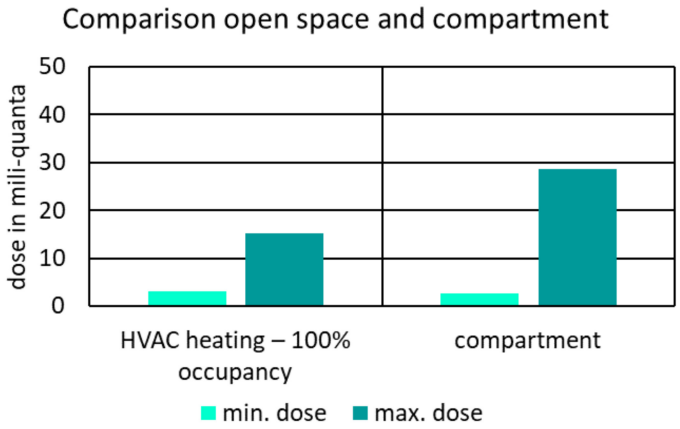

Figure 13. Comparison of the absorbed quanta dose in a large-capacity railcar (**left**) versus a compartment (**right**): min. dose, minimum dose absorbed farther away from the emitter; max. dose, maximum exposure that is absorbed close to the emitter.

3.5. Risk Assessment

In all cases, the highest protective effect is obtained by wearing an FFP2 mask by all passengers. This measure provides both good third-party protection and high self-protection. In addition, speaking loudly should be avoided. This represents another way of releasing as small an amount of infectious material as possible. Filtered recirculation reduces the emission load farther away from the emitter. In contrast, the load closer to the infected person decreases only slightly or may have a slightly higher concentration peak due to the associated reduction in airflow. Operation with pure fresh air at a lower total flowrate results in a higher concentration peak in the area of the emitter but reduces the exposure to passengers farther away. Since in reality the infected person remains unknown to fellow passengers, the highest possible level of self-protection is advisable for every passenger.

The comparison makes it clear that only the consistent use of an FFP2 mask can achieve values in the near and far range of the emitter in the lower range of the probability

of infection with the original SARS-CoV-2 virus reported from the observational study. Speaking loudly significantly increases exposure by a factor of about 28 and thus indirectly increases the theoretical risk of infection. The recommendation to avoid loud talking in all public transport as a risk-reduction measure can be justified because it is expected that this also worsens the fit of the mask [52]. In addition, masks should only be removed as briefly as possible for eating or drinking. Technical measures, such as increasing the fresh air rate or recirculating filtered air limit the area of spread and thus reduce the risk of infection farther away from the emitter.

A direct derivation from the level of exposure to a possible medical risk from the quanta dose determined in each case is not considered possible. However, Ref. [53] gives indications on the risk of infection in Chinese high-speed trains in the period December 2019 to March 2020. The study also distinguishes between exposure in the close range of the emitter and in the more distant range. The assumption is made that the Chinese high-speed trains are ventilated in a basically similar way to the German ICE trains. Thus, the risk of infection in the ICE can at least be classified. Due to cultural customs, it can at best be assumed that people in Chinese trains speak quietly and never loudly. Whether the Chinese passengers were wearing MNP at the time and to what extent cannot be determined. However, wearing MNP in public transport was quite common in Asia even before the pandemic. Therefore, the comparison can only serve as an orientation. Another limitation is that the study refers to the original SARS-CoV-2 variant. Over time, however, the apparently more contagious mutations dominate the infections. With these assumptions and limitations, the probability of infection can be narrowed down for the original SARS-CoV-2 in such a way that the risk of infection lies in the range of 0.14% to 3.5% when 0.6 to 40 mili-quanta are inhaled. For this purpose, the dose range (Figure 14) between "Breathing without MNP" and "Talking with MNP" for the HVAC heating case with high occupancy was colored in the diagram.

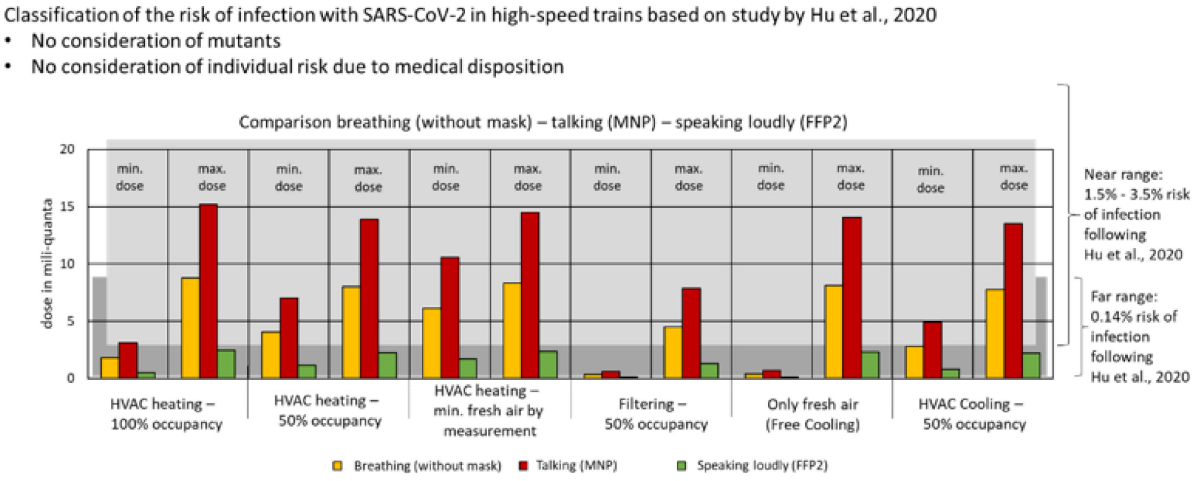

Figure 14. Comparison of the dose in mili-quanta determined in the simulation in the area farther away from the infected person compared to the determined probability of infection according to Hu et al. [53].

Assuming that the ventilation system is similar to the bus considered here, a comparison with documented contagions during bus trips indicates that a substantial risk of infection may exist. For example, during a 2.5 h bus ride, Ref. [54] described eight additional infections attributable to an infected person. The infected persons were both close to and farther away from the infected person. The authors of [55] investigated infections during a total 1 h 40 min pilgrimage of Buddhist believers in a bus. Here, 24 of 68 passengers later tested positive for SARS-CoV-2. Both studies indicate that the buses were ventilated with a recirculating air component. Since the studies consider individual

cases, it is not possible to make a generalized estimate of risk, as is the case for high-speed trains [53]. The studies do not include averages over several journeys or information on journeys with infected persons without contagions. Moreover, it cannot be excluded that the index persons were super emitters, i.e., their emission is higher by a factor of 10–100 than assumed in the simulations shown here. Thus, the exposure for other passengers would also have been correspondingly higher. Nevertheless, the studies impressively show that contagions cannot be ruled out even for the scenarios simulated here.

4. Results

Potential exposure to SARS-CoV-2 via aerosols is detailed for each mode of transportation in Section 3. Figures 15–17 compare the cases "breathing without mask", "speaking with MNP" and "speaking loudly with FFP2". The respective times spent in vehicles were estimated due to the lack of available data (Table 4). For the selection, a reference ventilation case or cases actually measured in operation were selected.

Figure 15 shows that, particularly in means of transport with a high proportion of recirculated air, an increased quanta dose can also be absorbed farther away from the emitter (min. dose). Near the emitter, this also applies to means of transport without recirculation. Figure 16 demonstrates that the combination "talking with MNP" leads to an increased exposure compared to "Breathing without mask". Figure 17 shows that even speaking loudly with an FFP2 mask results in a lower dose than breathing without a mask.

A significant reduction of the dose and thus of the risk results from the use of MNP or FFP2 masks, as well as from not speaking loudly. Refraining from loud speech leads to a reduction of the quanta emission of about 80%. The consistent wearing of an FFP2 mask by all passengers causes a reduction of the inhaled dose of 99%. If passengers use MNP, the reduction is only 65%. The zonal modeling approach can also be used to show that the location of the infectious passenger in relation to others plays a major role for the spread and exposure.

In addition, discrepancies between expected and actual ventilation were found in some measurements. The reduced supply of fresh air leads to a significantly higher infection risk, especially in the vicinity of the infected person.

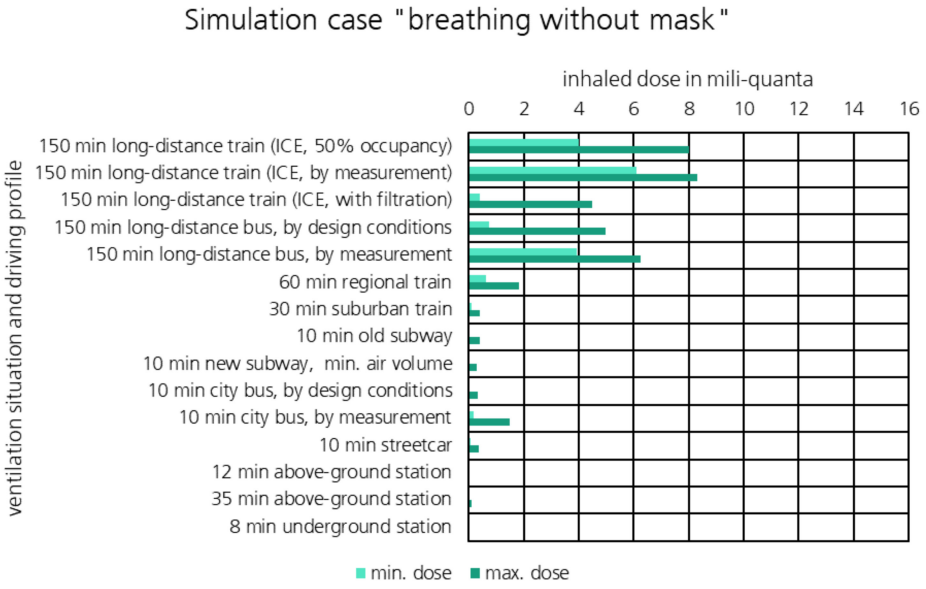

Figure 15. Comparison of typical means of transport considered for the case "breathing without mask": min. dose, minimum dose absorbed farther away from the emitter; max. dose, maximum exposure that is absorbed close to the emitter.

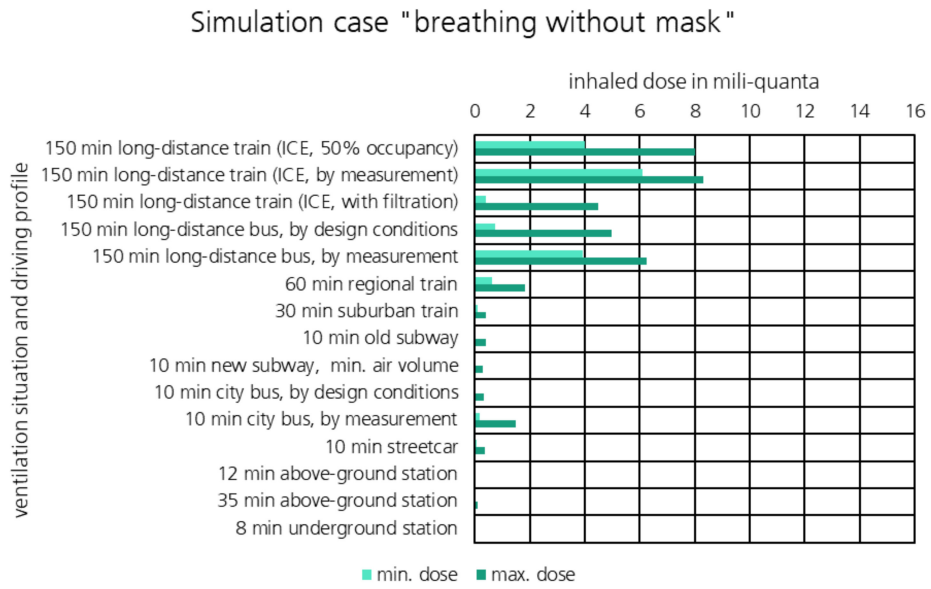

Figure 16. Comparison of typical means of transport considered for the case "Talking with MNP": min. dose, minimum dose absorbed farther away from the emitter; max. dose, maximum exposure that is absorbed close to the emitter.

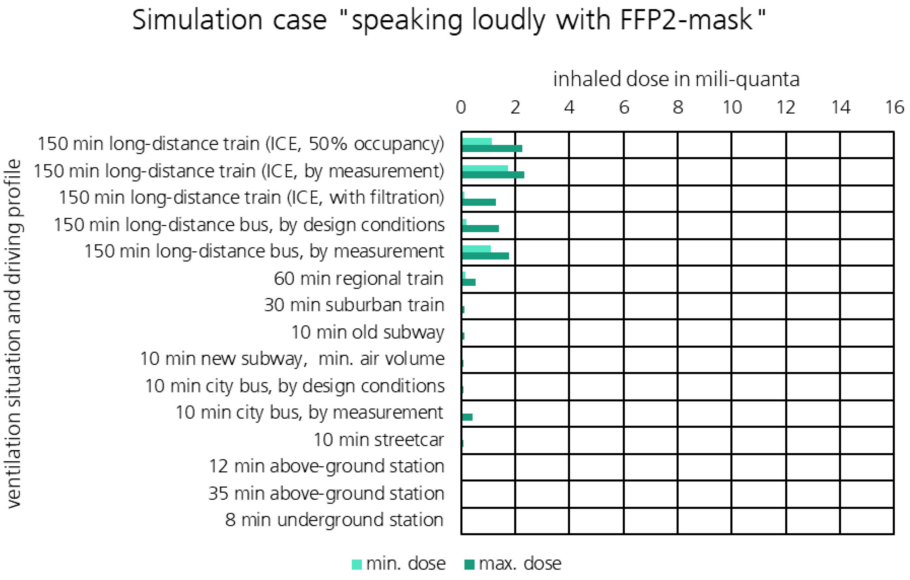

Figure 17. Comparison of typical means of transport considered for the case "Speaking loudly with FFP2": min. dose, minimum dose absorbed farther away from the emitter; max. dose, maximum exposure that is absorbed close to the emitter.

5. Discussion

This study deals with the risk of essentially airborne transmission of SARS-CoV-2 in public transport. The simulations allow the assessment of the potential exposure in the near and far field when travelling with an infected passenger. A direct conclusion from the exposure in a coach to a percentage risk, however, is not possible. An analogy comparison between the study from Hu et al. [53] on infections in Chinese high-speed trains and with the simulation results of the ICE from Section 3.3 provides at least an estimate. Through this analogy consideration, it is shown that there is also a risk of infection with SARS-CoV-2 when using rail- and road-passenger transport. This risk is different for different scenarios but can, to a large extent, be mitigated by technical measures such as recirculation air

filtration, increased fresh airflow and by personal behavior such as mask wearing and refraining from loud speech. For example, the highest theoretical risk of infection are for routes with a longer duration, no masks and loud speaking, as determined based on the comparatively high quanta dose. More infectious mutations of the Sars-CoV-2 virus and the vaccination or infection of large fractions of the populations have, to some extent, outdated the risk assessed by Hu [53]; nevertheless, the general conclusions of this simulation study remain valid.

For the exposure calculations, the quanta approach was chosen because this term does not attempt to model, for example, the flight dynamics of particles. From these calculations, it is evident that a significantly lower dose is achieved on the platforms of the stations investigated compared to the interior of the respective means of transport. On the one hand, this can be attributed to the relatively short stay of only a few minutes and on the other hand to the good ventilation. In accordance with the current scientific literature (e.g., [56]), no higher theoretical risk of infection is found in outdoor areas, in this case in the area of the train station hall. Provided that the minimum distance can be maintained, it is, therefore, possible to dispense with the wearing of an MNP or an FFP2 mask in outdoor areas.

In the confined areas, and if the required minimum distance cannot be maintained, there is a theoretical risk of infection. In these cases, further measures should be taken to reduce the risk, e.g., wearing a mask to prevent direct droplet infection. FFP2 masks show a higher reduction in both emission and inhaling of infectious material compared with surgical MNP. For this reason, they are more suitable for both third-party and self-protection.

5.1. Influence of Input Parameters

It should be taken into account that the study described here investigates the mean emission of a SARS-CoV-2 infected person during different activities (breathing, talking or speaking loudly) and using different masks (none, MNP or FFP2/N95). Here, it is always assumed that all passengers wear the same type of mask for the entire trip. Mixtures of mask types give results between the cases considered. So, for example, if the emitter has an MNP and the person taking in the dose has an FFP2 mask, the dose taken in can be expected to be between the "MNP" case and the "FFP2" case.

There are reports of so-called super emitters, who emit up to 100 times more than a normal emitter [57]. In the simulation, this would likewise lead to a factor of 100 higher dose uptake. In the case of the reported infections in public transport, it is unknown whether these are due to "normal" or super emitters. The impact of a super emitter in this simulation would be a factor of 100 higher; the relative ratios of the measures to each other would be unaffected.

5.2. Influence of Compliance

The simulations assume full compliance of rules by the passengers, i.e., the rules for wearing MNP or FFP2 and refraining from loud speech. Obviously, unruly passengers would lead to a situation closer to the case of no-mask with elevated speech in terms of source intensity and/or infectious matter uptake.

5.3. Influence of Occupancy

One limitation of this study is that the actual risk of presence of one infected passenger is not known. Thus, even though intuitively a higher occupation will result in higher risk of presence of an infected passenger, this cannot be quantified. Therefore, in demand-controlled ventilation cases, the trade-off between higher occupancy reducing airborne transmission due to increased ventilation and the increased risk that one of the passengers actually is infected is not possible.

Due to the lack of quantification, the occupancy density in the sense of the probability of the presence of a passenger infected with SARS-CoV-2 as a risk factor is thus not evaluated in this study.

6. Conclusions

The study investigates the theoretical risk for infection with SARS-CoV-2 in public transport using dispersion modeling in different vehicles and train stations. The actions (breathing, talking and speaking loudly), as well as the preventive measures (masks, filtering recirculating air and fresh air operation), are used to determine the risk assessment based on the definition of an infected passenger in the model. It is shown that the risk is reduced most efficiently if loud speaking is avoided and a FFP2 (N95) mask is worn correctly. Only these two measures create a reduction of the virus load of over 99% for both those in the close range of the infected person and those farther away. Thus, the already known protective measures, such as keeping quiet and using masks, can be confirmed in this study. Technical measures, such as recirculating filtered air further reduce the exposure to other passengers in the close range by 30–69% and farther away in the same vehicle by 80–91% (except in the streetcar/tram, where near-field exposure is increased by 17% due to filter-related reduced airflow). Higher fresh air rates also lead to a decrease in exposures in the broader environment. The study shows that near-field exposure cannot be eliminated, no matter how good the ventilation is. However, the refurbishment of trains and buses with HEPA filters in the recirculation air would lead to a clear reduction of other passengers' exposure. In addition, operators should absolutely avoid decreasing fresh air ventilation rates during operation. More broadly, these findings show that local protection can only be achieved locally (mask wearing), whereas central protection (filtration) mainly is effective more distant from the source. Hence, future research and development should focus on how technical solutions could act locally, for example by using partitions or ionization for the supply air. Analysis of the space needed to comply with the distance rules reveals that the distances cannot be met inside the vehicles. Therefore, the mask requirement should remain in place to protect against transmission by droplets. Compared with the risk inside the means of transport, the exposure on the platforms of the stations is considered minor. Particularly on above-ground platforms and provided that the recommended minimum distance of 1.5 m can be consistently maintained, the wearing of an MNP/FFP2 mask is temporarily dispensable, or an interruption of the mask requirement is justifiable. The inhaled quanta doses in the various means of transport mainly depend on the time spent in the vehicles. The ventilation of the transport vehicles also has an impact but is subordinate to the time component.

Even though new mutations of the SARS-CoV-2 virus and the increased immunity of large fractions of the population have altered the initial risk of infection, the general conclusions in this paper are considered valid.

Author Contributions: Conceptualization, C.M., V.N. and H.W.; methodology, V.N.; software, C.M.; validation, C.M.; formal analysis, V.N.; investigation, C.M. and V.N.; resources, T.H., B.N., M.S., A.S., M.E. and M.J.; data curation, T.H., B.N., M.S., A.S., M.E. and M.J.; writing—original draft preparation, C.M.; writing—review and editing, C.M. and V.N.; visualization, C.M. and V.N.; supervision, H.W.; project administration, H.W.; funding acquisition, H.W. All authors have read and agreed to the published version of the manuscript.

Funding: This research was funded by Deutsches Zentrum für Schienenverkehrsforschung beim Eisenbahnbundesamt grant number 2020-33-S-1202.

Institutional Review Board Statement: Not applicable.

Informed Consent Statement: No applicable.

Acknowledgments: This study was commissioned by "German Center for Rail Transport Research (DZSF) at the Railroad Federal Office". The authors are responsible for the content of this publication.

Conflicts of Interest: The authors declare no conflict of interest.

References

1. Scheuch, G. Breathing Is Enough: For the Spread of Influenza Virus and SARS-CoV-2 by Breathing Only. *J. Aerosol Med. Pulm. Drug Deliv.* **2020**, *33*, 230–234. [CrossRef] [PubMed]
2. Wang, C.C.; Prather, K.A.; Sznitman, J.; Jimenez, J.L.; Lakdawala, S.S.; Tufekci, Z.; Marr, L.C. Airborne transmission of respiratory viruses. *Science* **2021**, *373*, 3–5. [CrossRef] [PubMed]
3. Harrison, A.G.; Lin, T.; Wang, P. Mechanisms of SARS-CoV-2 Transmission and Pathogenesis. *Trends Immunol.* **2020**, *41*, 1100–1115. [CrossRef] [PubMed]
4. Hadei, M.; Hopke, P.K.; Jonidi, A.; Shahsavani, A. A Letter about the Airborne Transmission of SARS-CoV-2 Based on the Current Evidence. *Aerosol Air Qual. Res.* **2020**, *20*, 911–914. [CrossRef]
5. Morawska, L.; Cao, J. Airborne transmission of SARS-CoV-2: The world should face the reality. *Environ. Int.* **2020**, *139*, 1–2. [CrossRef] [PubMed]
6. Nazari, A.; Jafari, M.; Rezaei, N.; Arash-Azad, S.; Talati, F.; Nejad-Rahim, R.; Taghizadeh-Hesary, F.; Taghizadeh-Hesary, F. Effects of High-speed Wind, Humidity, and Temperature on the Generation of a SARS-CoV-2 Aerosol; a Novel Point of View. *Aerosol Air Qual. Res.* **2021**, *21*, 200574. [CrossRef]
7. Gameiro Da Silva, M. An analysis of the transmission modes of COVID-19 in light of the concepts of Indoor Air Quality. *REHVA J.* **2020**, *3*, 46–54. [CrossRef]
8. Statistisches Bundesamt. Korrektur: 46% Weniger Fahrgäste im Fernverkehr mit Bussen und Bahnen im 1. Halbjahr. 2020. Available online: https://www.destatis.de/DE/Presse/Pressemitteilungen/2020/10/PD20_424_461.html (accessed on 9 February 2022).
9. Tirachini, A.; Cats, O. COVID-19 and Public Transportation: Current Assessment, Prospects, and Research Needs. *JPT* **2020**, *22*. [CrossRef]
10. Kutela, B.; Novat, N.; Langa, N. Exploring geographical distribution of transportation research themes related to COVID-19 using text network approach. *Sustain. Cities Soc.* **2021**, *67*, 102729. [CrossRef]
11. Shen, J.; Duan, H.; Zhang, B.; Wang, J.; Ji, J.S.; Wang, J.; Pan, L.; Wang, X.; Zhao, K.; Ying, B.; et al. Prevention and control of COVID-19 in public transportation: Experience from China. *Environ. Pollut.* **2020**, *266*, 115291. [CrossRef]
12. Heinrich, J.; Zhao, T.; Quartucci, C.; Herbig, B.; Nowak, D. SARS-CoV-2 Infektionen während Reisen mit Bahn und Bus. Ein systematisches Review epidemiologischer Studien. *Gesundh. Bundesverb. Arzte Offentlichen Gesundh.* **2021**, *83*, 581–592. [CrossRef] [PubMed]
13. Arpino, F.; Grossi, G.; Cortellessa, G.; Mikszewski, A.; Morawska, L.; Buonanno, G.; Stabile, L. Risk of SARS-CoV-2 in a car cabin assessed through 3D CFD simulations. *arXiv* **2022**, arXiv:2201.09958.
14. Park, J.; Kim, G. Risk of COVID-19 Infection in Public Transportation: The Development of a Model. *Int. J. Environ. Res. Public Health* **2021**, *18*, 12790. [CrossRef]
15. Woodward, H.; Fan, S.; Bhagat, R.K.; Dadonau, M.; Wykes, M.D.; Martin, E.; Hama, S.; Tiwari, A.; Dalziel, S.B.; Jones, R.L.; et al. Air Flow Experiments on a Train Carriage—Towards Understanding the Risk of Airborne Transmission. *Atmosphere* **2021**, *12*, 1267. [CrossRef]
16. Will, H.; Scherer, C.; Stratbücker, S.; Norrefeldt, V.; Matheis, C.; Reith, A.; Schwitalla, C.; de Boer, J.; Neves Pimenta, D.; Zaglauer, M.; et al. Risikoeinschätzung zur Ansteckungsgefahr mit COVID-19 im Schienenpersonen—Sowie im Straßenpersonennah- und -Fernverkehr. Berichte des Deutschen Zentrums für Schienenverkehrsforschung, Nr. 12, Dresden. 2021. Available online: https://www.dzsf.bund.de/SharedDocs/Textbausteine/DZSF/Forschungsberichte/Forschungsbericht_2021-12.html (accessed on 9 February 2022).
17. Norrefeldt, V.; Grün, G.; Sedlbauer, K. VEPZO—Velocity propagating zonal model for the estimation of the airflow pattern and temperature distribution in a confined space. *Build. Environ.* **2012**, *48*, 183–194. [CrossRef]
18. Modelica Association. Modelica. Available online: https://modelica.org/ (accessed on 7 February 2022).
19. Hartmann, A.; Lange, J.; Rotheudt, H.; Kriegel, M. Emissionsrate und Partikelgröße von Bioaerosolen beim Atmen, Sprechen und Husten. 2020. Available online: https://do.tu-berlin.de/bitstream/11303/11451/4/hartmann_etal_2020_de.pdf (accessed on 9 February 2022).
20. Pathak, A.; Norrefeldt, V.; Lemouedda, A.; Grün, G. The Modelica Thermal Model Generation Tool for Automated Creation of a Coupled Airflow, Radiation Model and Wall Model in Modelica. In Proceedings of the 10th International Modelica Conference, Lund, Sweden, 10–12 March 2014; Linköping University Electronic Press: Linköping, Sweden, 2014; pp. 115–124.
21. Buonanno, G.; Morawska, L.; Stabile, L. Quantitative assessment of the risk of airborne transmission of SARS-CoV-2 infection: Prospective and retrospective applications. *Environ. Int.* **2020**, *145*, 106–112. [CrossRef] [PubMed]
22. Buonanno, G.; Stabile, L.; Morawska, L. Estimation of airborne viral emission: Quanta emission rate of SARS-CoV-2 for infection risk assessment. *Environ. Int.* **2020**, *141*, 105794. [CrossRef]
23. Müller, D.; Rewitz, K.; Derwein, D.; Burgholz, T.M.; Schweiker, M.; Bardey, J.; Tappler, P. *Abschätzung des Infektionsrisikos durch Aerosolgebundene Viren in Belüfteten Räumen (2. Überarbeitete und Korrigierte Auflage)*; RWTH Aachen Uviersity: Aachen, Germany, 2021.
24. Jimenez, J.L. *SARS-CoV-2 Aerosol Transmission Estimator*; University of Colorado: Boulder, CO, USA, 2020.
25. Asadi, S.; Wexler, A.S.; Cappa, C.D.; Barreda, S.; Bouvier, N.M.; Ristenpart, W.D. Aerosol emission and superemission during human speech increase with voice loudness. *Sci Rep.* **2019**, *9*, 2348. [CrossRef] [PubMed]

26. Edwards, D.A.; Man, J.C.; Brand, P.; Katstra, J.P.; Sommerer, K.; Stone, H.A.; Nardell, E.; Scheuch, G. Inhaling to mitigate exhaled bioaerosols. *Proc. Natl. Acad. Sci. USA* **2004**, *101*, 17383–17388. [CrossRef]
27. RWTH Aachen University. RisiCo. Available online: https://risico.eonerc.rwth-aachen.de/ (accessed on 15 February 2022).
28. Lahrz, T.; Bischof, W.; Sagunski, H.; Baudisch, C.; Fromme, H.; Grams, H.; Gabrio, T.; Heinzow, B.; Müller, L. Gesundheitliche Bewertung von Kohlendioxid in der Innenraumluft. Mitteilungen der Ad-hoc-Arbeitsgruppe Innenraumrichtwerte der Innenraumlufthygiene-Kommission des Umweltbundesamtes und der Obersten Landesgesundheitsbehörden. *Bundesgesundheitsblatt Gesundh. Gesundh.* **2008**, *51*, 1358–1369. [CrossRef]
29. Howard, J.; Huang, A.; Li, Z.; Tufekci, Z.; Zdimal, V.; van der Westhuizen, H.-M.; Von Delft, A.; Price, A.; Fridman, L.; Tang, L.-H.; et al. An evidence review of face masks against COVID-19. *Proc. Natl. Acad. Sci. USA* **2021**, *118*. [CrossRef] [PubMed]
30. Grinshpun, S.A.; Haruta, H.; Eninger, R.M.; Reponen, T.; McKay, R.T.; Lee, S.-A. Performance of an N95 filtering facepiece particulate respirator and a surgical mask during human breathing: Two pathways for particle penetration. *J. Occup. Environ. Hyg.* **2009**, *6*, 593–603. [CrossRef] [PubMed]
31. Davies, A.; Thompson, K.-A.; Giri, K.; Kafatos, G.; Walker, J.; Bennett, A. Testing the efficacy of homemade masks: Would they protect in an influenza pandemic? *Disaster Med. Public Health Prep.* **2013**, *7*, 413–418. [CrossRef]
32. Nordquist, B. Vädring av Skolor—Ett Komplement till Normal Ventilation? Ph.D. Thesis, Department of Building Science, Lund Institute of Technology, Lund, Sweden, 1998.
33. Deutscher Wetterdienst. Testreferenzjahre (TRY). 2021. Available online: https://www.dwd.de/DE/leistungen/testreferenzjahre/testreferenzjahre.html (accessed on 9 February 2022).
34. Deutsche Bahn, AG. Daten & Fakten. 2019. Available online: https://assets.static-bahn.de/dam/jcr:1289cfc8-512e-42c3-a7e3-04302f1784c7/233600-311901.pdf (accessed on 9 February 2022).
35. Deutsche Bahn, AG. Kennzahlen der DB Regio nach Geschäftsbereichen. Available online: https://www.dbregio.de/wir/zahlen-daten-fakten (accessed on 9 February 2022).
36. Deutsche Bahn, AG. Züge im Fernverkehr: Zugtypen und Ihre Strecken: ICE 4. Available online: https://www.bahn.de/p/view/service/zug/fahrzeuge/zugtypen.shtml?dbkanal_007=L01_S01_D001_KIN_-rs-zug_NAVIGATION-fahrzeuge_LZ01 (accessed on 9 February 2022).
37. Schwandl, R. *Tram Atlas Deutschland 5*, 5th ed.; Revidierte Ausgabe; Robert Schwandl: Berlin, Germany, 2019; ISBN 9783936573602.
38. Maibaum, C.-A. Strassenbahn-Online. Available online: http://www.strassenbahn-online.de/ (accessed on 9 February 2022).
39. Esser, B. Tram-info. Available online: https://www.tram-info.de/ (accessed on 9 February 2022).
40. Verband Deutscher Verkehrsunternehmen VDV. VDV-Statistik & Jahresbericht. Available online: https://www.vdv.de/statistik-jahresbericht.aspx (accessed on 9 February 2022).
41. Stade, C. Gleispläne der Webseite gleisplanweb.de. Available online: https://gleisplanweb.eu/ (accessed on 9 February 2022).
42. Deutsche Bahn, AG. Produktmanagement ICE: Fahrzeuglexikon für den Fernverkehr. Available online: http://download-data.deutschebahn.com/static/datasets/fahrzeuglexikon/Fahrzeuglexikon_2017.pdf (accessed on 9 February 2022).
43. Siemens, A.G. Der Icx—Eine Neue Ära im Fernverkehr der Deutschen Bahn. Available online: https://docplayer.org/37850426-Siemens-com-mobility-der-icx-eine-neue-aera-im-fernverkehr-der-deutschen-bahn.html (accessed on 9 February 2022).
44. Scharff, S. Markteinführung des TALENT 3 mit Ausblick. In *Sonderheft Graz*; Statistisches Amt: Graz, Austria, 2017; p. 141.
45. Vlexx GmbH. Datenblatt Bombardier Talent 3. Available online: https://www.vlexx.de/ueber-uns/fahrzeugflotte/talent3/ (accessed on 9 February 2022).
46. EvoBus GmbH. Die Citaro Stadtbusse. *Technische Information*. Available online: https://www.mercedes-benz-bus.com/de_DE/buy/services-online/download-technical-brochures.html#content/headline_840766654_c (accessed on 9 February 2022).
47. HeiterBlick GmbH. TW3000 Hannover Datenblatt. Available online: https://www.heiterblick.de/fahrzeuge/hochflur/tw-3000/ (accessed on 9 February 2022).
48. Münchner Verkehrsgesellschaft mbH. Website der Münchner Verkehrsgesellschaft mbH (MVG). Available online: https://www.mvg.de/ (accessed on 9 February 2022).
49. Norta, M.; Valleé, D. Ein Verkehrsmittelwahlmodell für den Personenfernverkehr auf der Basis von Verkehrswiderständen. Ph.D. Thesis, University of Aachen, Aachen, Germany, 2012.
50. Kebdani, Z. Ventilation of subway stations. Personal communication, 2021.
51. DIN—Deutsches Institut für Normung e.V. *DIN EN 14750-1*; Bahnanwendungen—Luftbehandlung in Schienenfahrzeugen des Innerstädtischen und Regionalen Nahverkehrs—Teil 1: Behaglichkeitsparameter; Deutsches Institut für Normung: Berlin, Germany, 2006.
52. Schumann, L.; Lange, J.; Rotheudt, H.; Hartmann, A.; Kriegel, M. Experimentelle Untersuchung der Leckage und Abscheideleistung von typischen Mund-Nasen-Schutz und Mund-Nasen-Bedeckungen zum Schutz vor luftgetragenen Krankheitserregern, Berlin. 2020. Available online: https://www.depositonce.tu-berlin.de/handle/11303/11975 (accessed on 9 February 2022).
53. Hu, M.; Lin, H.; Wang, J.; Xu, C.; Tatem, A.J.; Meng, B.; Zhang, X.; Liu, Y.; Wang, P.; Wu, G.; et al. Risk of Coronavirus Disease 2019 Transmission in Train Passengers: An Epidemiological and Modeling Study. *Clin. Infect. Dis.* **2021**, *72*, 604–610. [CrossRef] [PubMed]

54. Luo, K.; Lei, Z.; Hai, Z.; Xiao, S.; Rui, J.; Yang, H.; Jing, X.; Wang, H.; Xie, Z.; Luo, P.; et al. Transmission of SARS-CoV-2 in Public Transportation Vehicles: A Case Study in Hunan Province, China. *Open Forum Infect. Dis.* **2020**, *7*, ofaa430. [CrossRef]
55. Shen, Y.; Li, C.; Dong, H.; Wang, Z.; Martinez, L.; Sun, Z.; Handel, A.; Chen, Z.; Chen, E.; Ebell, M.H.; et al. Community Outbreak Investigation of SARS-CoV-2 Transmission Among Bus Riders in Eastern China. *JAMA Intern. Med.* **2020**, *180*, 1665–1671. [CrossRef]
56. Qian, H.; Miao, T.; Liu, L.; Zheng, X.; Luo, D.; Li, Y. Indoor transmission of SARS-CoV-2. *Indoor Air* **2021**, *31*, 639–645. [CrossRef]
57. Moreno, T.; Pintó, R.M.; Bosch, A.; Moreno, N.; Alastuey, A.; Minguillón, M.C.; Anfruns-Estrada, E.; Guix, S.; Fuentes, C.; Buonanno, G.; et al. Tracing surface and airborne SARS-CoV-2 RNA inside public buses and subway trains. *Environ. Int.* **2021**, *147*, 106326. [CrossRef]